

Photo-patterned hybrid gels as first-generation shaped enzyme bioreactors

Phillip R. A. Chivers,^a Jamie A. Kelly,^a Max J. S. Hill^a and David K. Smith^a

a: Department of Chemistry, University of York, Heslington, York, YO10 5DD, UK

Contents

1. Materials and methods
2. Macromolecule diffusion
3. Solution-phase studies
4. Qualitative ALP activity tests
5. Enzyme leaching experiments
6. Gel characterisation
7. ALP bioreactors
8. Substrate/product uptake studies
9. NMR study
10. AP bioreactor
11. References

1. Materials and methods

NMR spectra were recorded on a Jeol ECX 400 (^1H 400 MHz, ^{13}C 100 MHz) spectrometer using D_2O as solvent. The chemical shifts are reported in parts per million (ppm) relative to tetramethylsilane as an external standard for ^1H NMR spectra and calibrated against the solvent residual peak. Positive ion ESI and MALDI mass spectra were recorded on a Bruker solarix FTMS 9.4T mass spectrometer. UV-vis absorbance spectroscopy was recorded on Shimadzu UV-2401 PC and Shimadzu UV-1800 spectrophotometers. Fluorescence spectroscopy was recorded on a Hitachi F-4500 fluorimeter, with emission and excitation slit widths both set to 2.5 nm. Rheological measurements were recorded using a Malvern Instruments Kinexus Pro+ rheometer fitted with a parallel plate geometry and data were processed using rSpace software. ATR-FTIR spectra were recorded on a PerkinElmer Spectrum Two FT-IR spectrometer. Melting points were measured on a Stuart SMP3 melting point apparatus and are uncorrected. SEM was carried out on freeze-dried samples sputtered with gold/palladium on a JEOL JSM-7600F FEG-SEM (Biology Technology Facility, University of York). Microscope parameters are provided alongside the corresponding image.

Synthesis of DBS- CO_2Me . DBS- CO_2Me was synthesised as described in the literature¹ – improved characterisation is provided here. D-Sorbitol (4.90 g, 26.90 mmol, 95% purity, VWR) was weighed into a 3-neck round bottom flask fitted with Dean-Stark apparatus. Cyclohexane (35 mL) and methanol (10 mL) were added and the mixture was stirred under N_2 at 50°C for 20 min. 4-Methylformylbenzoate (7.50 g, 45.69 mmol, 98.5% purity, Alfa Aesar) and p-toluenesulfonic acid hydrate (1.00 g, 5.80 mmol, 99% purity, Acros Organics) were dissolved in methanol (20 mL) and stirred for 20 min at room temperature and added dropwise to the reaction mixture. The reaction temperature was raised to 70°C and the mixture stirred for a further 2 h, topping up with 1:1 cyclohexane:methanol as required. The white paste formed was washed with methanol (3×100 mL) before drying under high vacuum for 2 h. The crude product was washed further with boiling water (5×100 mL) and boiling DCM (3×100 mL) to remove mono- and tri- substituted derivatives respectively. The clean product was dried *in vacuo*. Yield 8.00 g (74%). M.p: $209\text{--}215^\circ\text{C}$; lit. $210\text{--}213^\circ\text{C}$.¹ ^1H NMR (400 MHz, DMSO-d_6): δ 8.00 (2H, d, $J=8$ Hz, Ar-H), 7.97 (2H, d, $J=8$ Hz, Ar-H), 7.62 (2H, d, $J=8$ Hz, Ar-H), 7.59 (2H, d, $J=8$ Hz, Ar-H), 5.76 (s, Ar-CH, 2H), 4.93 (d, CH-OH, $J=6$ Hz, 1H), 4.47 (br, CH_2OH , 1H), 4.24 (1H, dd, $J=2,13$ Hz, COCHH'), 4.22 (1H, dd, $J=2,9$ Hz, CHCHCH), 4.18 (1H, dd, $J=2,13$ Hz, COCHH'), 4.01 (1H, br, $\text{CH}_2\text{CH}(\text{O})\text{CH}$), 3.89 (1H, dd, $J=2,9$ Hz, CHCHCHOH), 3.85 (6H, s, CH_3), 3.79 (1H, br, CHOH), 3.62 (1H, br d, $J=12$ Hz, CHH'OH), 3.47 (1H, br d, CHH'OH). ^{13}C NMR (100 MHz, DMSO-d_6): 166.01 (COO), 143.34 (aromatic p-C), 143.07 (aromatic p-C), 129.77 (aromatic o-C), 129.72 (aromatic o-C), 129.04 (aromatic, m-H), 128.95 (aromatic, m-H), 126.51 (aromatic, m-H), 98.53 (Ph-C), 98.45 (Ph-C), 77.58 (CH), 70.18 (CH), 69.31 (CH_2), 68.53 (CH), 67.58 (CH), 62.56 (CH_2), 52.21 (CH_3). ν_{max} (cm^{-1}): 3251w, 2956w, 1983w, 1724s, 1276s, 1093s, 1018s, 854m, 750s. ESI-MS (m/z) calc. for $\text{C}_{24}\text{H}_{26}\text{O}_{10}\text{Na}$ 497.1424; found 497.1424 (100% $[\text{M}+\text{Na}]^+$).

Synthesis of DBS-CONHNH $_2$. The synthesis of DBS-CONHNH $_2$ was carried out as previously reported¹ – improved characterisation is provided here. DBS- CO_2Me (1.10 g, 2.32 mmol) was weighed into a round-bottomed flask and dissolved in THF (40 mL). Hydrazine monohydrate (6.19 g, 12 mmol, 98% purity, TCI) was added to the reaction mixture, which was stirred under reflux at 70°C for 16 h. Upon reaction completion (monitored by TLC) the white precipitate formed was filtered and washed with deionised water (3×100 mL). The product was dried first under high vacuum, then in a vacuum oven at 80°C to constant mass. The final product was ground to yield a white powder. Yield 1.01 g (92%). ^1H NMR (400 MHz, DMSO-d_6): δ 9.81 (s, CONHNH $_2$, 2H), 7.82 (2H, d, $J=8$ Hz, Ar-H), 7.81 (2H, d, $J=8$ Hz, Ar-H), 7.53 (2H, d, $J=8$ Hz, Ar-H), 7.50 (2H, d, $J=8$ Hz, Ar-H), 5.71 (s, Ar-CH, 2H), 4.95 (d, CH-OH, $J=6$ Hz, 1H), 4.51 (s, CONHNH $_2$, 4H), 4.47 (1H, dd, $J=6,6$ Hz, CH_2OH), 4.22 (1H, dd, $J=2,13$ Hz, COCHH'), 4.19

(1H, dd, J=2,9 Hz, CHCHCH), 4.17 (1H, dd, J=2,13 Hz, COCHH'), 3.98 (1H, ddd, J=1,1,2 Hz, CH₂CH(O)CH), 3.87 (1H, dd, J=2,9 Hz, CHCHCHOH), 3.77 (1H, dddd, J=2,6,6,6 Hz, CHOH), 3.62 (1H, ddd, J=2,6,12, CHH'OH), 3.47 (1H, ddd, J=2,6,12 Hz, CHH'OH). ¹³C NMR (100 MHz, DMSO-d₆): 165.67 (C=O), 141.30 (aromatic p-C), 141.03 (aromatic p-C), 133.56 (aromatic o-C), 133.47 (aromatic o-C), 126.81 (aromatic, m-H), 126.73 (aromatic, m-H), 126.13 (aromatic, m-H), 126.10 (aromatic, m-H), 98.80 (Ph-C), 98.73 (Ph-C), 77.60 (CH), 70.16 (CH), 69.37 (CH₂), 68.51 (CH), 67.69 (CH), 62.62 (CH₂). ν_{\max} (cm⁻¹): 3295s, 2881w, 1569m, 1091s. ESI-MS (m/z) calc. for C₂₂H₂₇O₈N₄ 475.1829; found 475.1823 (100% [M+H]⁺).

Synthesis of PEGDM. The synthesis of PEGDM was carried out as described in the literature.² PEG 8000 (8.00 g, 1.00 mmol, 95% purity, Fisher Scientific), was dissolved in dry DCM (15 mL) and stirred at room temperature with methacrylic anhydride (0.34 g, 2.2 mmol, 94% purity, Alfa Aesar) and triethylamine (0.2 mL, 0.15 mmol) over activated molecular sieves (3.00 g, 3 Å sieve) for 4 days. The solution was filtered over alumina, which was washed with further DCM (*ca.* 100 mL). The product was then precipitated by addition of diethyl ether. The product was filtered and dried under high vacuum to yield a white solid. Yield 6.10 g (75%). M.p: 58-60°C; lit. 59-61°C.² ¹H NMR (400 MHz, CDCl₃): δ 6.13 (s, =CH, 4H), 5.57 (t, =CH, J=2, 2H), 4.29 (t, OCH₂, J=5, 4H), 3.83-3.44 (m, polymer chain OCH₂, 620H), 1.94 (s, CH₃, 6H). ¹³C NMR (100 MHz, CDCl₃): δ 175.03 (COO), 135.91 (C=CH₂), 125.63 (C=CH₂), 70.36 (OCH₂), 68.91 (OCH₂), 63.69 (OCH₂), 18.15 (CH₃). ν_{\max} (cm⁻¹): 2881s, 1716w, 1466m, 1341m, 1279w, 1241w. MALDI-MS (m/z): M_n = 6138.00 \equiv (C₄H₅O_{1.5})₂(C₂H₄O)₁₃₆.

2. Macromolecule diffusion

An aqueous solution of either 50 μ M fluorescein or fluorescein-isothiocyanate-dextran (M_w from 4-70 kDa) was pipetted on top of the gel sample and the fluorescence after excitation (λ_{exc} = 470 nm) monitored at the λ_{max} of the fluorophore solution as recorded at 50 μ M. Control experiments in the absence of fluorophore were carried out for comparison. The emission and excitation slit widths were set to 2.5 nm in all cases.

Quantification was achieved by comparison to calibration curves. Decreasing fluorescence intensity at greater fluorophore concentrations – caused by increasing optical density of the solution - was compensated for using a calculation reported by Lakowicz:³

$$F_{\text{corr}} \cong F_{\text{obs}} \cdot 10^{\frac{OD_{\text{exc}} + OD_{\text{em}}}{2}}$$

Where F_{corr} is the corrected fluorescence intensity, F_{obs} is the observed fluorescence intensity, and the optical density of the sample at the emission and excitation wavelengths are OD_{em} and OD_{exc} respectively.

Table S1: Physical characteristics of the fluorophores used in this study. Absorption maxima (recorded at 50 μ M), calculated Stokes radius and literature gyration radius values for each compound.

Fluorophore	λ_{max} nm	Calculated Radius nm	Gyration Radius ⁴ Nm
Fluorescein	512	-	-
FITC-dextran (3-5 kDa)	521	1.50	2.0
FITC-dextran (10 kDa)	522	2.28	-
FITC-dextran (20 kDa)	526	3.14	3.4
FITC-dextran (40 kDa)	528	4.32	5.0
FITC-dextran (70 kDa)	521	5.59	6.3

3. Solution-phase studies

Bovine intestinal ALP (2 μL , 21.6 U μL^{-1} , from Sigma) was dissolved in buffer solution or water (1.998 mL) to give a stock solution of concentration 21.6 U mL^{-1} . This was further diluted as required.

A UV cuvette was charged with a known volume of ALP stock solution. This solution was diluted to 2 mL with pNPP disodium salt hexahydrate (pNPP, $M_w = 371.14 \text{ g mol}^{-1}$) such that the final concentrations of ALP and pNPP were known. The formation of pNP was monitored by UV-vis spectroscopy at the maximum absorbance of the product in the given solvent. The solvents used the maximum absorbance values in each are:

- pH 4 citrate buffer (0.1 M): $\lambda_{\text{max}} = 310 \text{ nm}$
- pH 7 phosphate buffer (0.2 M): $\lambda_{\text{max}} = 310 \text{ nm} + 405 \text{ nm}$
- pH 9 glycine-NaOH buffer (0.2 M): $\lambda_{\text{max}} = 405 \text{ nm}$
- pH 11 carbonate buffer (0.1 M): $\lambda_{\text{max}} = 405 \text{ nm}$
- Unbuffered water: $\lambda_{\text{max}} = 310 \text{ nm} + 405 \text{ nm}$

UV-vis spectra were also recorded at various time points in the range 250 – 450 nm. Concentrations of pNPP and pNP were calculated by comparison of the experimental absorbances to those of calibration curves in each solvent.

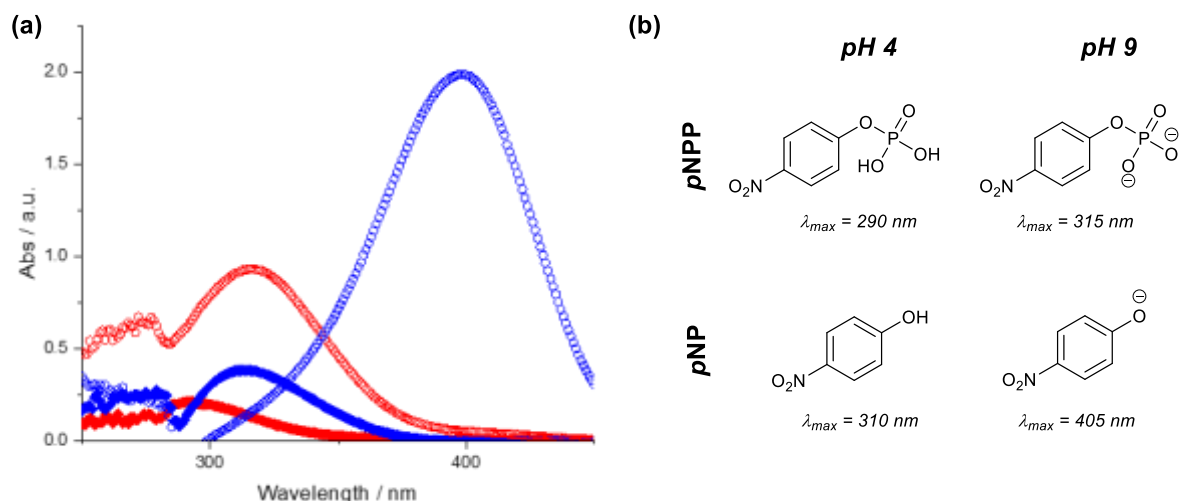


Fig. S1: UV spectra of pNPP (solid) and pNP (hollow) at pH 4 (red) and pH 9 (blue). All spectra recorded at a concentration of 0.016 mM (a). Structures and absorption maxima of pNPP and pNP at pH 4 and pH 9 (b).

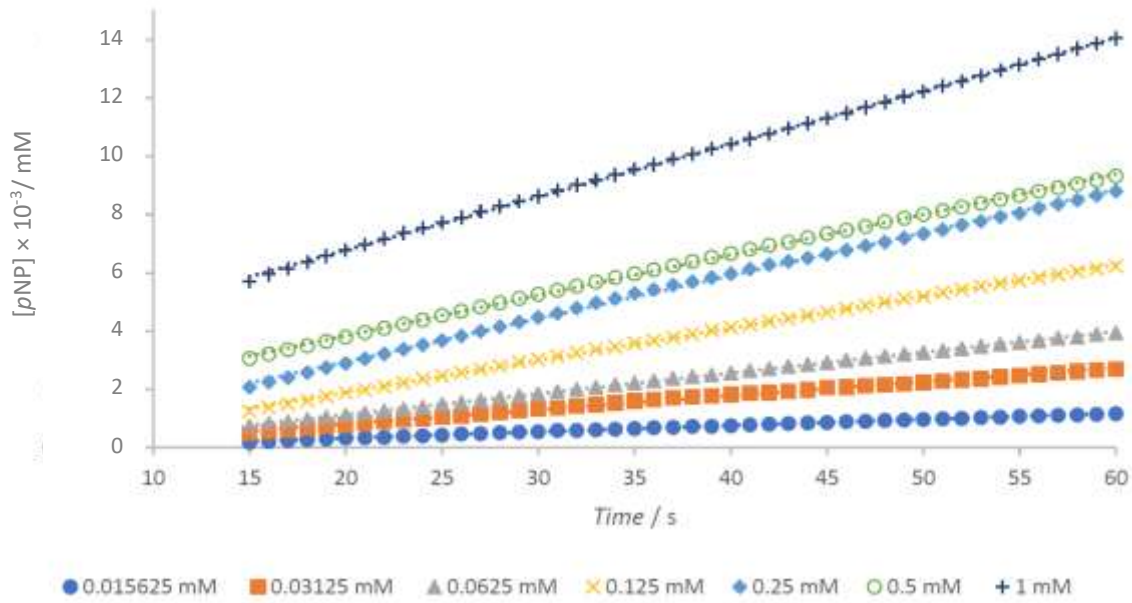


Fig. S2: Representative changes in ALP-catalysed pNP formation over time at different substrate concentrations. ALP concentration was 0.1 U mL^{-1} for all samples.

From the rates of pNPP hydrolysis, it was possible to derive the Michaelis constant (K_m) and the maximum velocity (V_{max}) under these reaction conditions. Under basic conditions, the rate of hydrolysis is determined by the enzyme-phosphate decomplexation kinetics, such that a general equation for the reaction can be considered as:



Where E = enzyme (ALP), S = substrate (pNPP) and P = product (pNP). The enzyme-substrate complex, ES, is assumed to be in a quasi-steady state, as the rate of its formation greatly exceeds that of decomplexation. Given this assumption, the rate of formation of product can be given as:

$$\frac{dP}{dt} = \frac{k_{cat}[E]_0[S]}{K_M + [S]}$$

Here, K_M is considered to be the concentration of substrate at which the reaction velocity is half of V_{max} . The maximum velocity is equivalent to the product of the concentration of enzyme and the rate constant of catalysis (k_{cat}). This equation can therefore be rewritten as:

$$V_0 = V_{max} \left(\frac{[S]}{K_M + [S]} \right)$$

V_0 is defined as the initial rate of product formation (i.e. dP/dt). Taking the gradient of each line in Fig. S2 and plotting it against the initial concentration of pNPP, a so-called Michaelis-Menten⁵ plot can be generated (Fig. S3).

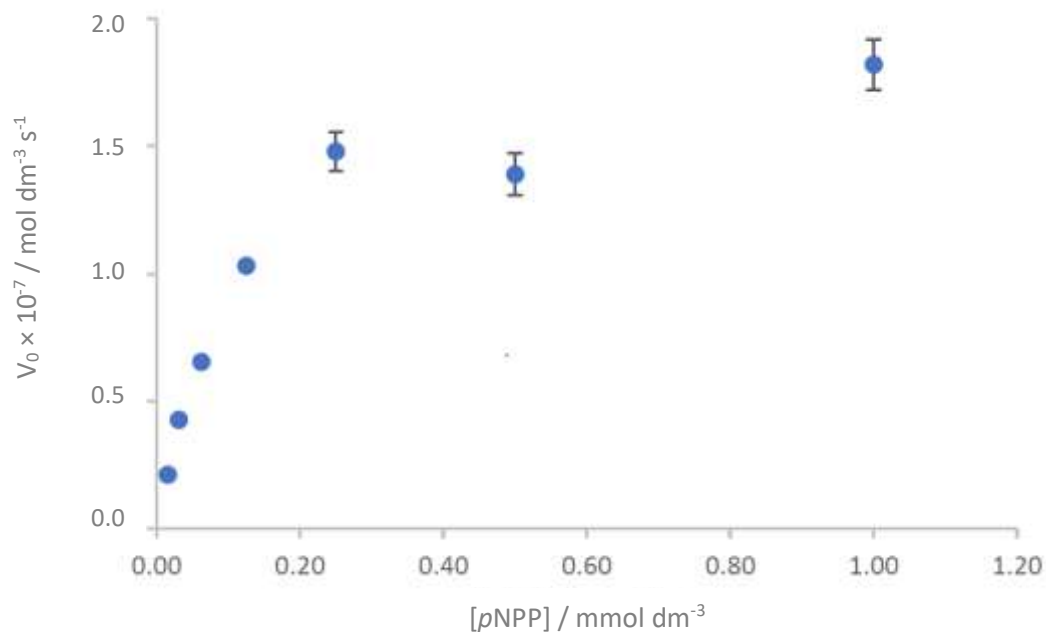


Fig. S3: Michaelis-Menten kinetic plot for the hydrolysis of pNPP using ALP at a concentration of 0.1 U mL⁻¹. Error bars represent one standard deviation and where not seen are smaller than the data points ($n = 3$).

An initial increase in the rate of pNPP hydrolysis is seen with increasing substrate concentration. The rate of pNP formation does begin to plateau at concentrations greater than 0.25 mM, likely due to saturation of the active sites of ALP. Above this concentration the reaction rate is limited by the decomplexation of enzyme and substrate. To generate values for K_M and V_{max} , the double reciprocal of Equation 4.4 (Equation 4.5) was plotted in what is known as a Lineweaver-Burk plot (Fig. S4).

$$\frac{1}{V_0} = \frac{K_M}{V_{max}} \cdot \frac{1}{[S]} + \frac{1}{V_{max}}$$

From this plot K_M and V_{max} can be calculated from the inverse of the x and y intercepts respectively. The values of these parameters are 0.14 mM and 2.1×10^{-4} mM s⁻¹ respectively, in relatively good agreement with literature values.⁶

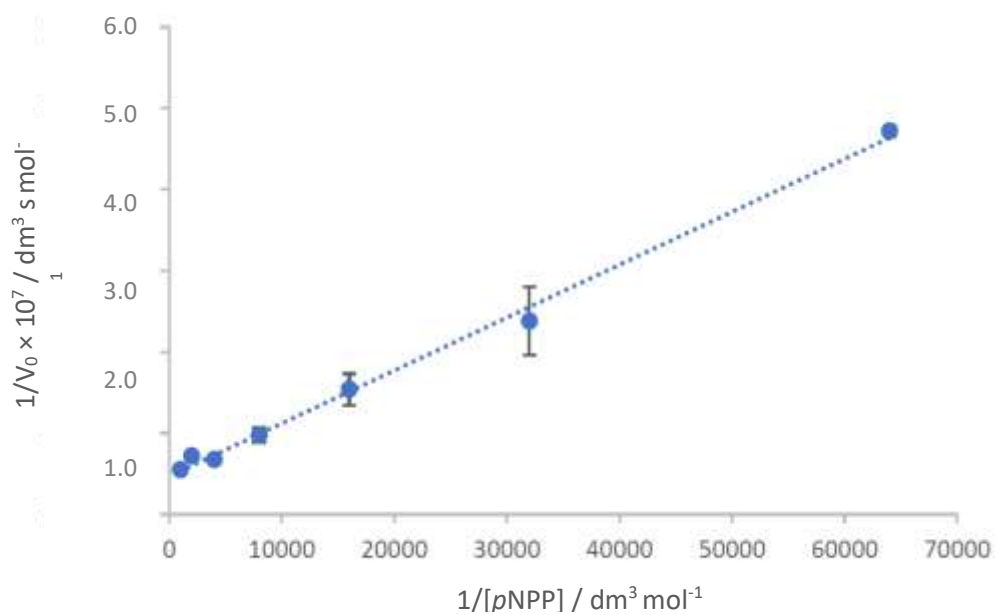


Fig. S4: Lineweaver-Burk plot for the hydrolysis of pNPP using ALP at a concentration of 0.1 U mL^{-1} . Error bars represent one standard deviation and where not seen are smaller than the data points ($n = 3$).

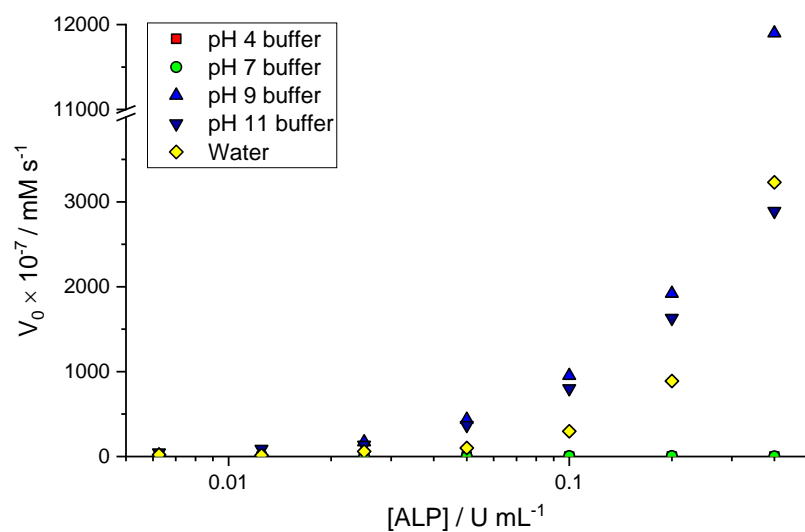


Fig. S5: Change in the initial rate of hydrolysis of pNPP (0.1 mM) with ALP concentration.

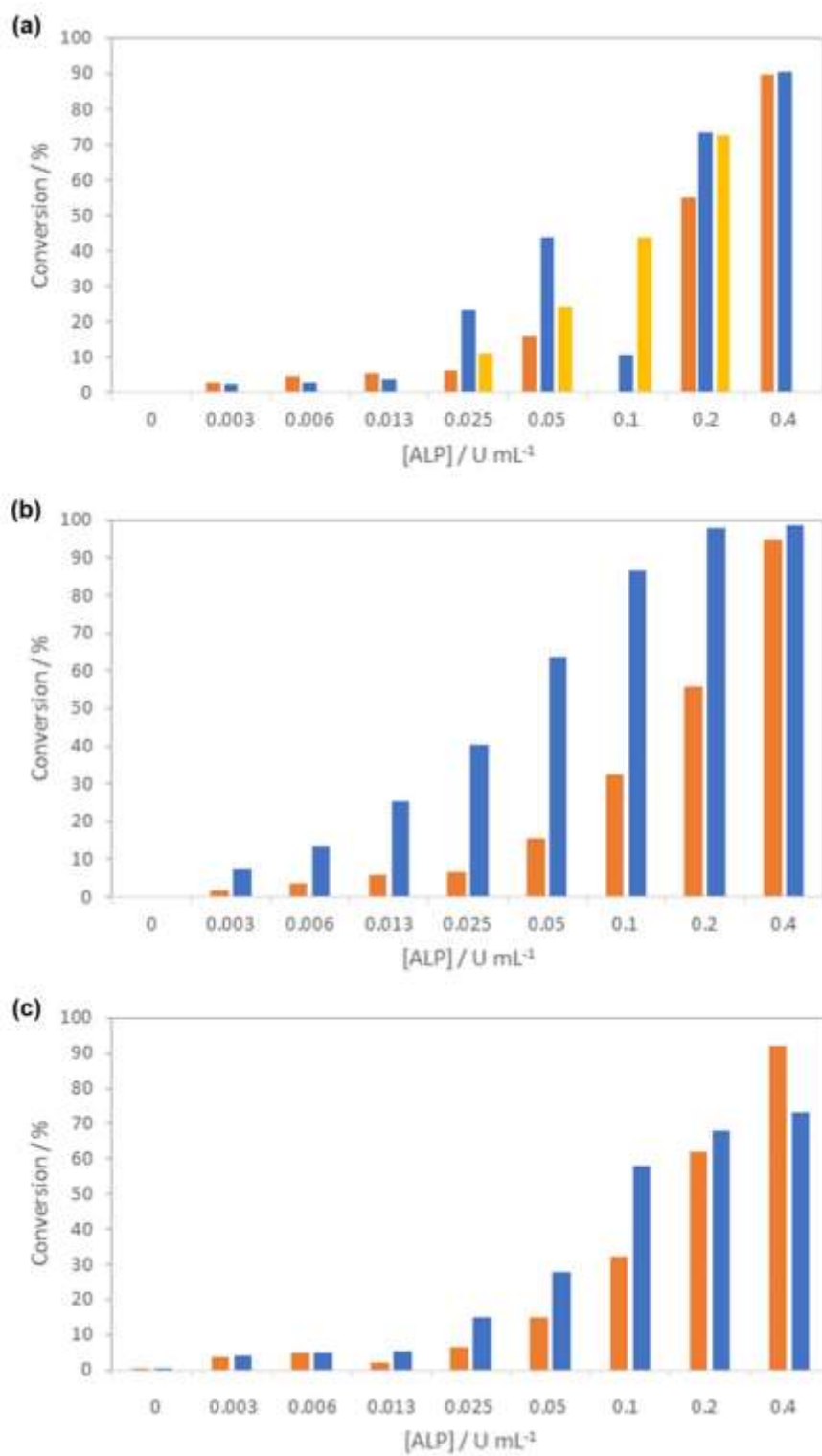


Fig. S6: Total conversion of pNPP over time at different concentrations of ALP in pH 9 buffer (a), pH 11 buffer (b) and in unbuffered water (c). Orange bars = 2 h, blue bars = 24 h, yellow bars = 48 h.

4. Qualitative ALP activity tests

All ALP activity tests were carried out using 10 mM *p*NPP solution (0.5 mL) made up in pH 9 glycine/NaOH buffer (0.2 M). Gels were washed once with water prior to addition of substrate.

ALP solutions were treated as required followed by mixing with *p*NPP solution.

DBS-CONHNH₂ gels were prepared by suspending DBS-CONHNH₂ (1.42 mg) in either H₂O or pH 9 buffer (0.5 mL). The suspension was sonicated (15 min) followed by heating to dissolution. On cooling a gel formed. *p*NPP solution was then pipetted on top.

For ALP-containing LMWGs, DBS-CONHNH₂ gels were prepared as described above, but on dissolution the vial was placed in a thermoregulated oil bath at a known temperature. After 5 min the vial was removed and ALP (1 μ L, 0.2 U μ L⁻¹) was added (ALP concentration in gel = 0.4 U mL⁻¹). For slow cooling, the vial was replaced in the oil bath and the cooling rate set to a known speed. For rapid cooling, the vial was placed immediately into an ice bath. On rapid cooling, gelation occurs. These gels were allowed to warm to room temperature before evaluating enzyme activity by pipetting *p*NPP solution on top.

For ALP-containing hybrid gels, the above procedure was followed until gelation. Following gel formation, a solution (0.5 mL) of PEGDM (10% wt/vol) and PI (0.5% wt/vol) was added on top and left for 3 days. After this time the supernatant was removed and the gel cured under a long-wavelength UV lamp (30 min) to initiate formation of the PG. *p*NPP solution was then pipetted on top.

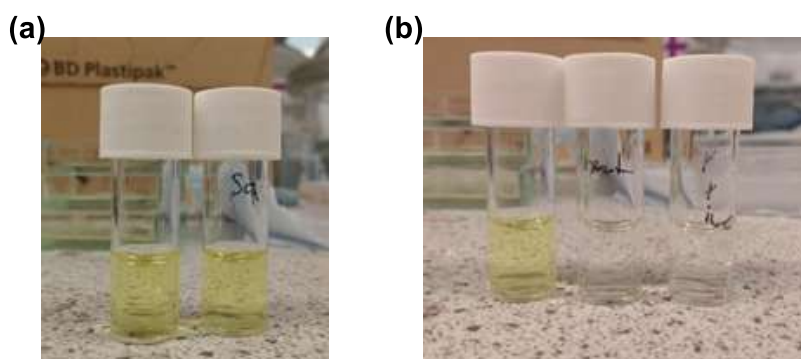


Fig. S7: Solution-phase studies of gelation stimuli on the bioactivity of ALP (0.2 U mL⁻¹). Activity in the hydrolysis of *p*NPP (5 mM) was tested in response to sonication (a: left = control, right = sample) and heat (b: left = control, middle = heated, right = heated and cooled in ice).

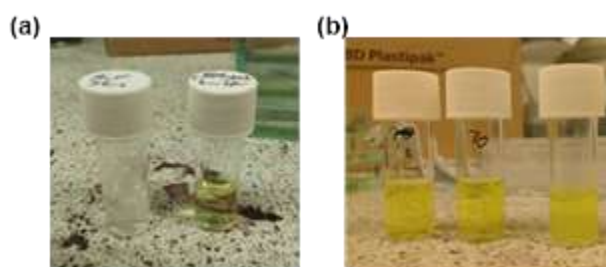


Fig. S8: Gel-phase studies of gelation stimuli on the bioactivity of ALP (0.4 U mL^{-1} in each gel). All gels are $6 \text{ mM DBS-CONHNH}_2$. Gel prepared by standard DBS-CONHNH₂ procedure (a: left = sample, right = control). Gels prepared by holding the hot sol at 80°C (b: left = untreated solution control, middle = treated solution control, right = gel injected with ALP).



Fig. S9: Effect of UV light on the bioactivity of ALP in solution (0.2 U mL^{-1}). Control (left), 0.5 h UV exposure (middle) and 0.5 h UV exposure in $0.05\% \text{ wt/vol PI}$ solution (right). $p\text{NPP}$ concentration was 5 mM in all cases.

5. Enzyme leaching experiments

Gels were prepared in a UV cuvette at a total volume of 2 mL . A solution of $\text{pH } 9$ buffer (2 mL) was pipetted on top of the gel. After 24 h the supernatant was removed and diluted to 4 mL with a 0.2 mM solution of $p\text{NPP}$ (final $p\text{NPP}$ concentration = 0.1 mM). The evolution of $p\text{NPP}$ was monitored over time using UV-vis spectroscopy by recording the absorbance at 405 nm . The rate of change in $p\text{NPP}$ concentration was compared to those from the solution phase studies (see above) at 0.1 mM $p\text{NPP}$ concentration. The rate of evolution was correlated to an ALP concentration, which was considered to be the approximate concentration of enzyme in the solution (i.e. leached enzyme).

Table S2: Calculated percentage ALP release from each gel type into $\text{pH } 9$ buffer. Errors given as standard deviation ($n = 3$).

Gel	Wash 1 release %	Wash 2 release %	Wash 3 release %	Total release %
DBS-CONHNH ₂	0.59	0.01	0.00	0.60
PEGDM	0.04	0.00	0.00	0.04
Hybrid	0.06	0.00	0.01	0.07

6. Gel characterisation

6.1. Electron Microscopy

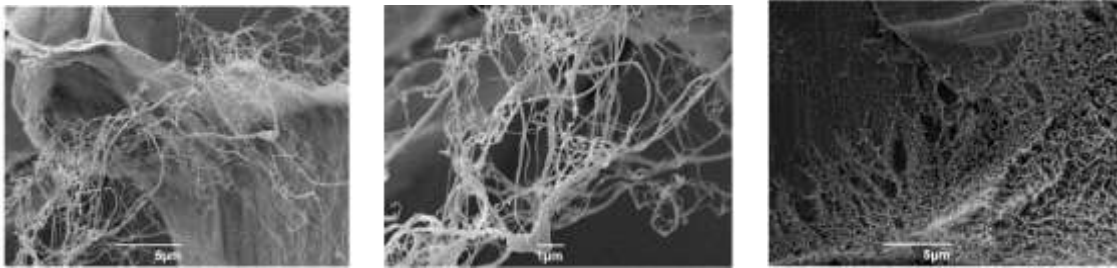


Fig. S10: SEM images of ALP-loaded DBS-CONHNH₂ gel at x 5,000 (left) and x 10,000 (middle) magnification. SEM of AP-loaded hybrid gel at x 5,000 magnification (right).

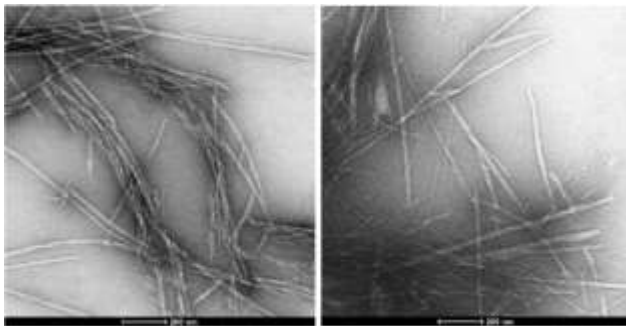


Fig. S11: TEM images of ALP-loaded (left) and AP-loaded (right) DBS-CONHNH₂ gels at x 30,000 magnification.

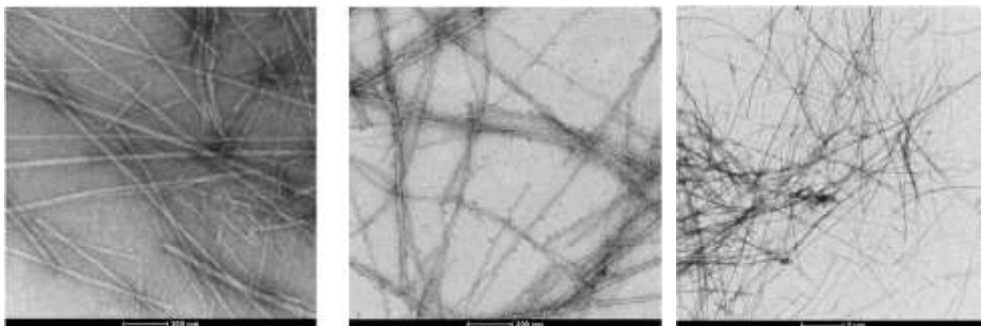


Fig. S12: TEM images of ALP-loaded (left) and AP-loaded (middle) hybrid gels at x 30,000 magnification. (Right) TEM image of AP-loaded hybrid gel at x 2,900 magnification.

6.2. Rheology

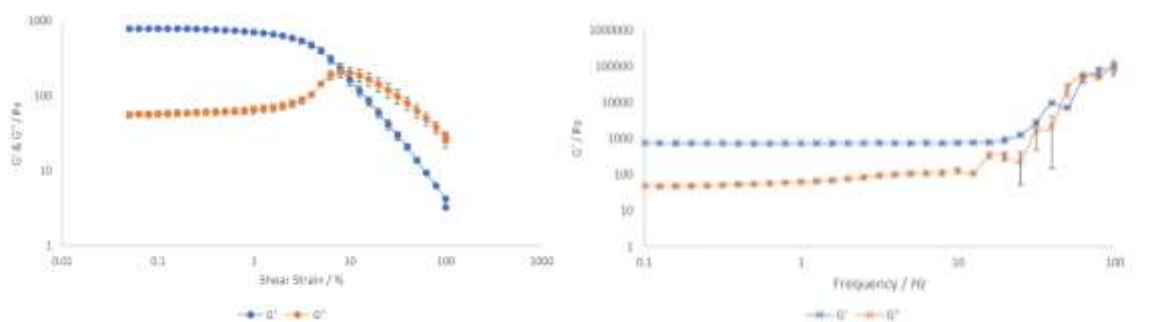


Fig. S13: Rheological traces of DBS-CONH NH_2 (6 mM) hydrogel. Amplitude (left) and frequency (right) sweeps.

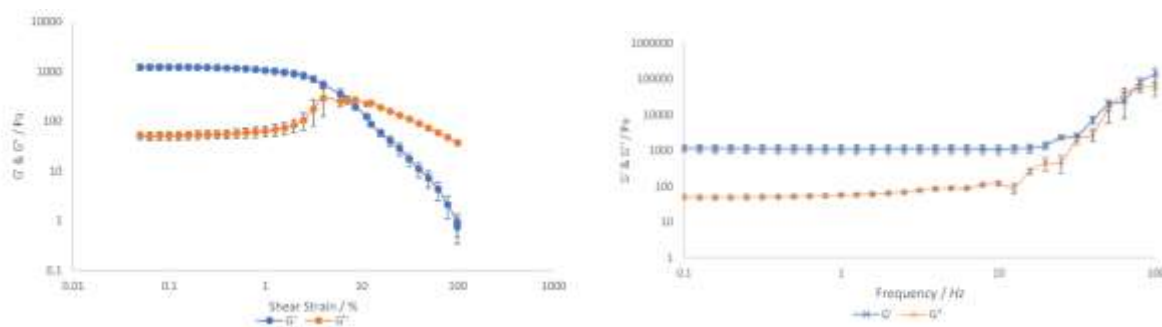


Fig. S14: Rheological traces of ALP-loaded DBS-CONH NH_2 (6 mM) hydrogel. Amplitude (left) and frequency (right) sweeps.

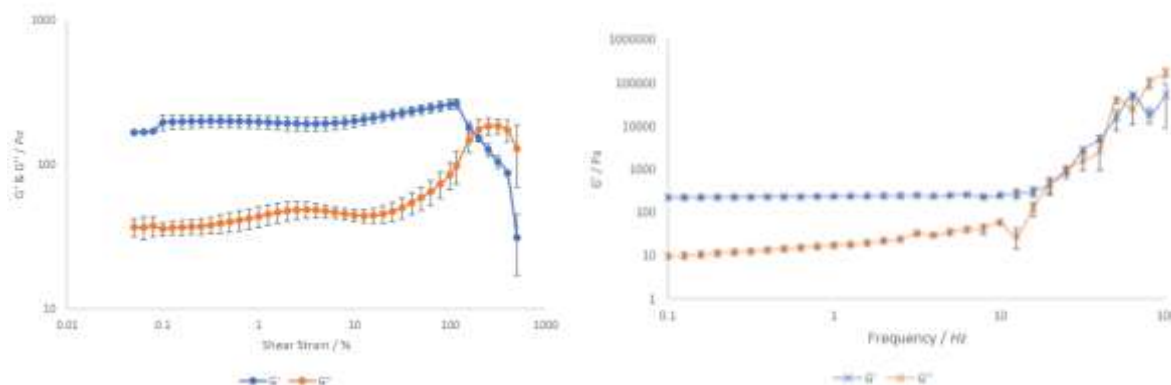


Fig. S15: Rheological traces of PEGDM (10% wt/vol) hydrogel. Amplitude (left) and frequency (right) sweeps.

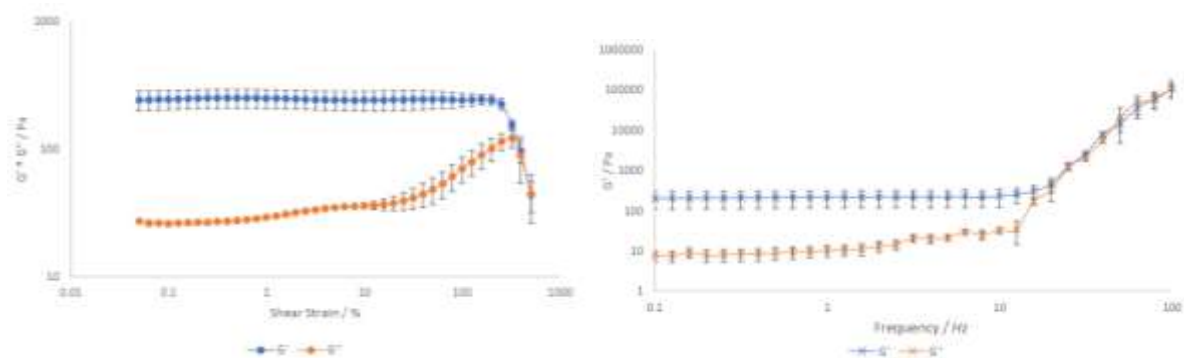


Fig. S16: Rheological traces of ALP-loaded PEGDM (10% wt/vol) hydrogel. Amplitude (left) and frequency (right) sweeps.

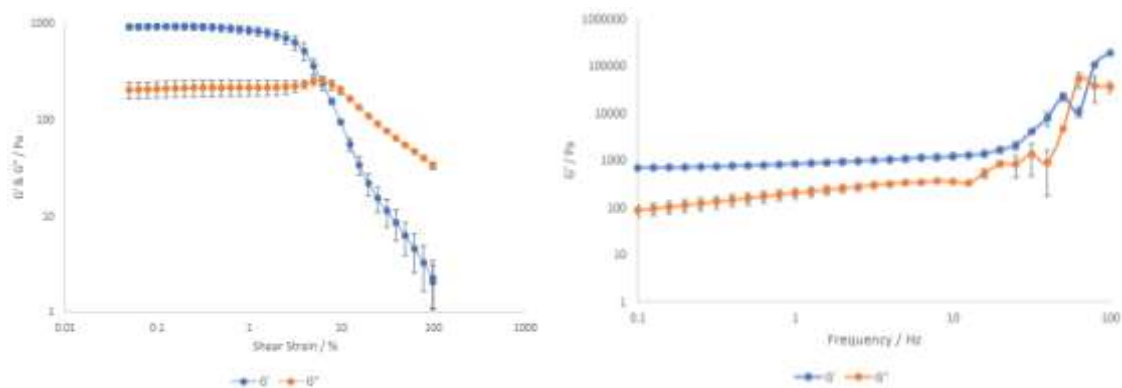


Fig. S17: Rheological traces of 10% hybrid hydrogel. Amplitude (left) and frequency (right) sweeps.

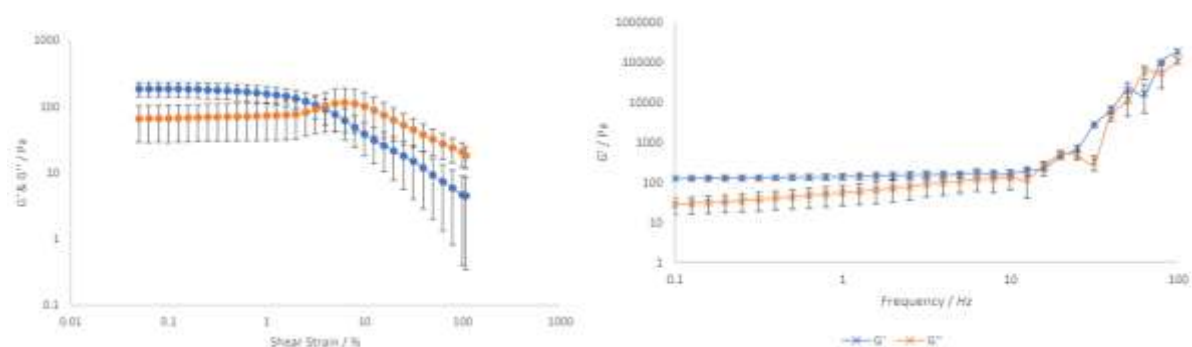


Fig. S18: Rheological traces of ALP-loaded 10% hybrid hydrogel. Amplitude (left) and frequency (right) sweeps.

6.3 IR Spectroscopy of dried xerogels

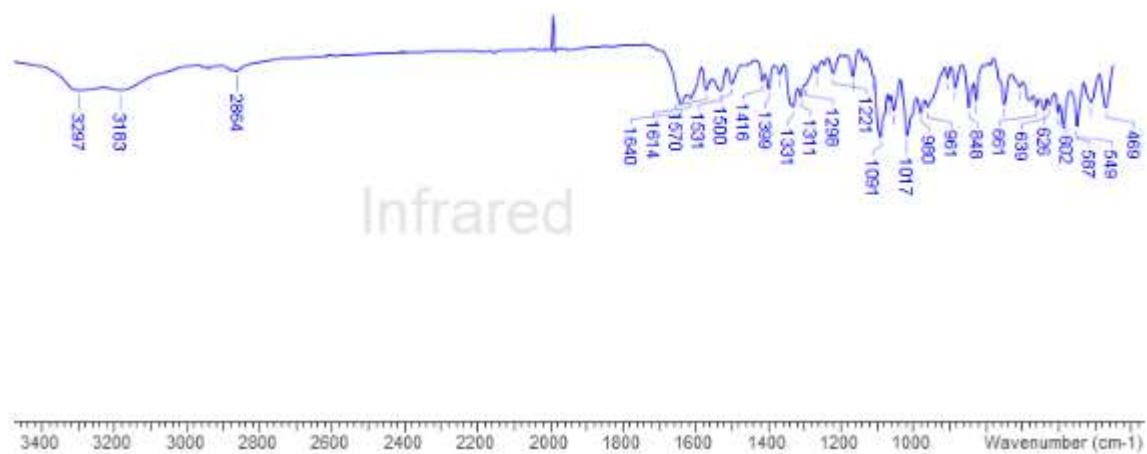


Fig. S19: IR spectrum of 6 mM DBS-CONHNH₂ gel.

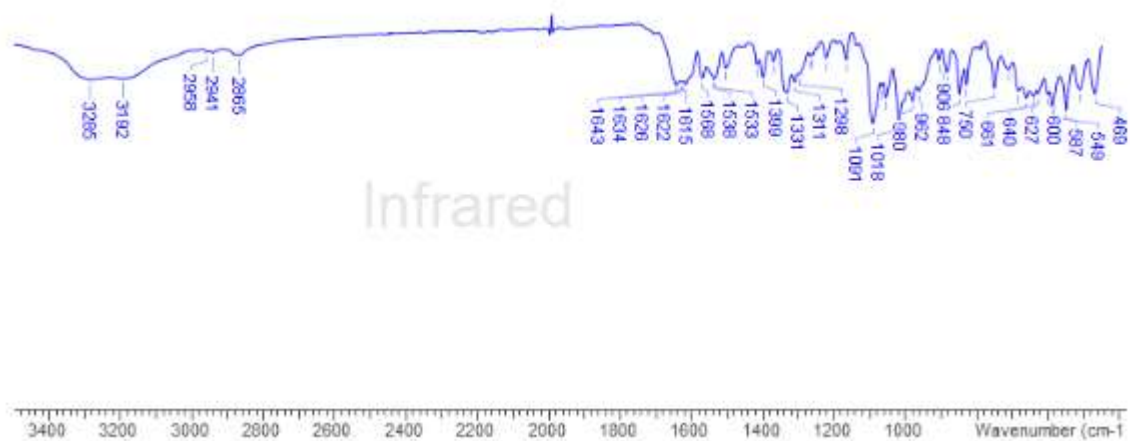


Fig. S20: IR spectrum of ALP-loaded 6 mM DBS-CONHNH₂ gel.

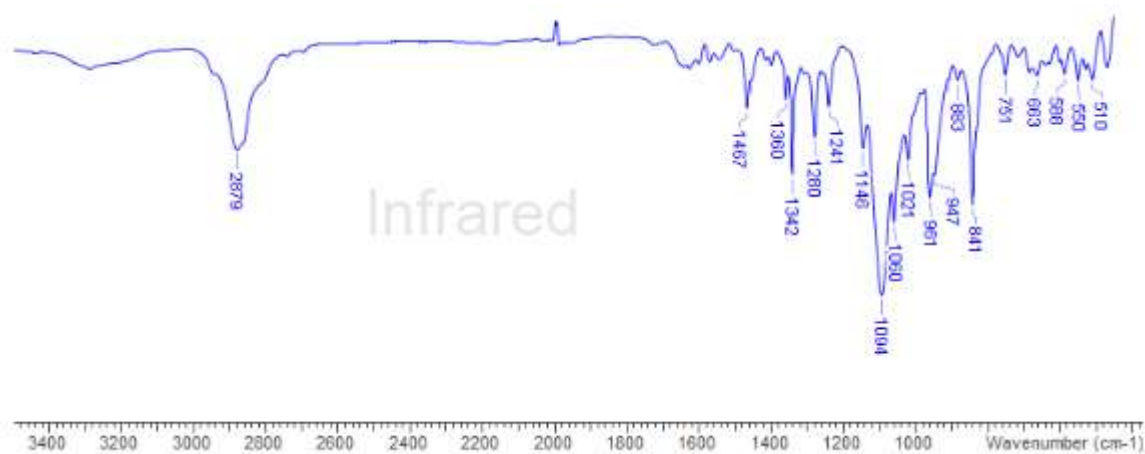


Fig. S21: IR spectrum of 10% hybrid gel

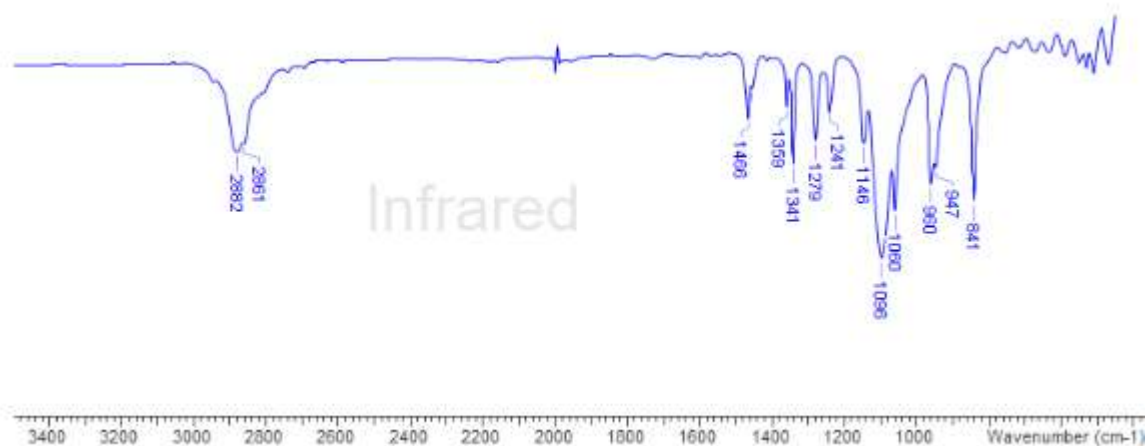


Fig. S22: IR spectrum of ALP-loaded 10% hybrid gel

7. ALP Bioreactors

7.1. Immobilised ALP

DBS-CONHNH₂ (28.4 mg) was dissolved in DMSO (0.4 mL) with sonication. This solution was mixed with boiling H₂O (9.6 mL) and the flask placed in a thermoregulated oil bath at 80 °C. The sample was left to equilibrate at this temperature for 5 min, at which point ALP solution (20 µL, 0.2 U µL⁻¹) was added (final ALP concentration = 0.4 U mL⁻¹). The hot solution was transferred immediately to a glass tray (5 cm × 5 cm × 1 cm) cooled in ice. Rapid gel formation was observed on cooling. Onto this gel was added a 10 mL solution of PEGDM (10% wt/vol) and PI (0.05% wt/vol). The sample was left for three days, then the supernatant was removed, and acetate photomasks placed over the top of the gel, such that only a ring-shaped section was exposed. The tray was placed in ice to minimise heating effects and irradiated with long-wavelength UV light (0.5 h). In this time, the exposed region had formed a robust hybrid gel. The remaining, soft LMW hydrogel was washed away using a low-pressure water jet to reveal the ring pattern.

The central compartment of the reactor was loaded with a solution of *p*NPP (0.3 mL, 10 mM) in pH 9 buffer. The outer compartment was charged with pH 9 buffer (2 mL). The whole reactor was placed in a dark container to prevent light-induced *p*NPP degradation. The outer compartment was stirred for the duration of the experiment. At each time point, the contents of the outer compartment were removed, placed in a UV cuvette, and the UV spectrum of the solution recorded. This solution was returned to the outer compartment after each measurement.

After 6 h, in addition to the removal of the buffer solution, the contents of the central compartment were pipetted into a UV-vis cuvette and diluted to 2 mL with pH 9 buffer. This solution was also analysed by UV-vis spectroscopy. Calibration curves plotted from absorbances of known concentrations of *p*NP and *p*NPP in pH 9 buffer were used to calculate the concentration of these compounds in each compartment.

7.1. Free ALP

A hybrid gel ring was fabricated as described in a previous report.¹ The compartment contained within the ring was charged with a solution of *p*NPP in pH 9 buffer (0.3 mL, 10 mM), whilst the outer compartment contained ALP dissolved in pH 9 buffer (26 U mL⁻¹, 2 mL). The whole reactor was placed in a dark container to prevent light-induced *p*NPP degradation. The outer compartment was stirred for the duration of the experiment. Analysis of the contents of each compartment was carried out as outlined above. Results were compared to a control reactor with no ALP. The diffusion of *p*NPP through to the outer compartment was recorded as described above.

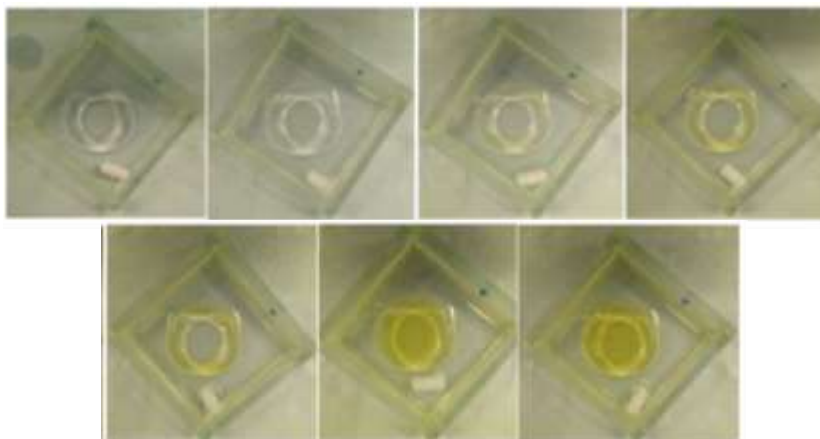


Fig. S23. Photographs of the reactor with ALP present in the 'product' compartment taken every 30 min from 0 h (top left) to 3 h (bottom right), showing the accumulation of yellow product within the gel ring.

8. Substrate/product uptake studies

Hydrogels of 2 mL volume were prepared in 8 mL vials as described previously. Solutions of *p*NP and *p*NPP were prepared in pH 4, 7 and 11 buffer solutions, at a concentration of 1 mM, and each was pipetted on top of a hydrogel. The samples were left for 24 h, after which time 2 mL of the solution was removed and analysed by UV-vis spectroscopy, before returning to the sample vial. This process was repeated at 48 h. Each combination of pH, gel and solution-phase component was tested in triplicate.

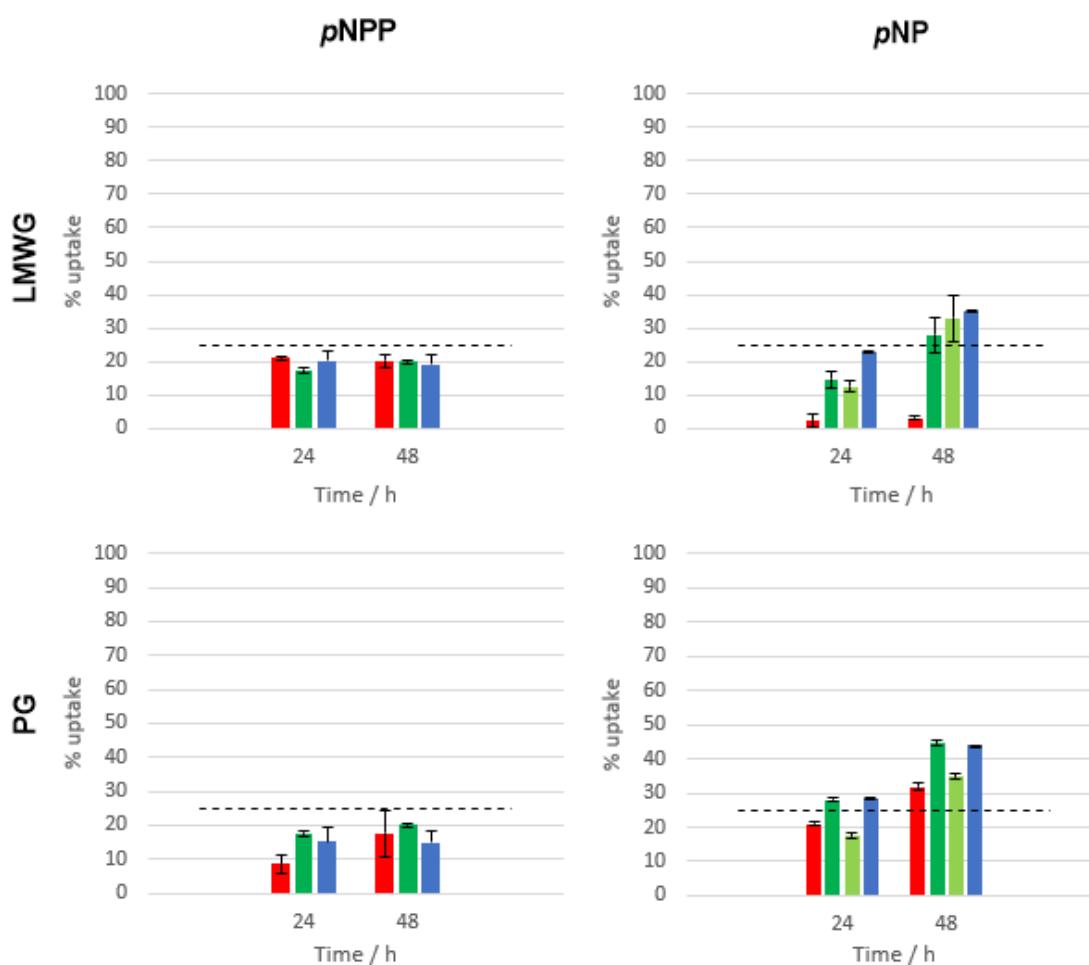


Fig. S24: Uptake of pNPP (left) and pNP (right) into DBS-CONHNNH₂ (top) and 10% PEGDM (bottom) hydrogels. Red bars = pH 4, blue bars = pH 11. Green bars are uptakes at pH 7. For pNP two distinct species are observed by UV at pH 7. The protonated and deprotonated forms are denoted by the dark and light green bars respectively. The dashed black line represents 25% uptake, the expected dilution based solely on equilibration of concentration. Errors given as standard deviation ($n = 3$).

9. NMR study

DBS-CONHNNH₂ (1.99 mg) was suspended in a solution of pNP (0.01 M) dissolved in D₂O (0.7 mL) containing 28 μ L DMSO as internal standard (0.56 M). The suspension was sonicated (15 min) and heated to dissolution. The hot sol was transferred to an NMR tube and allowed to cool under ambient conditions. A gel formed quickly in the NMR tube. Standard ¹H NMR of the gel was performed.

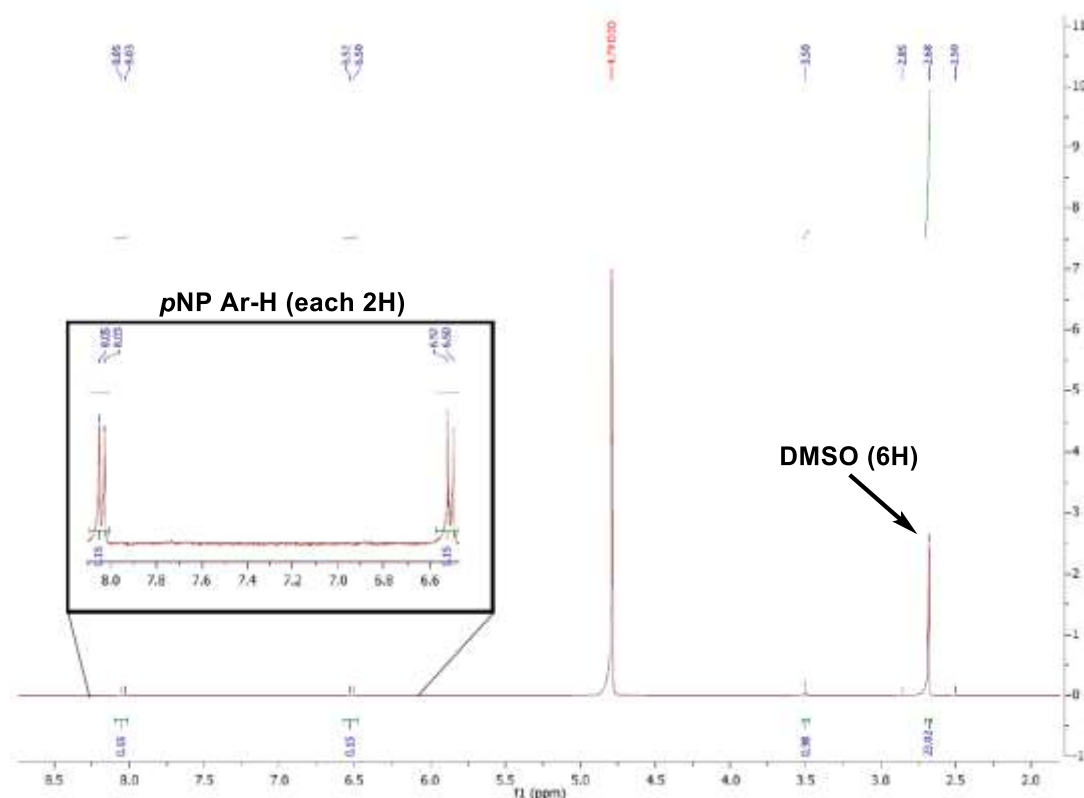


Fig. S25: NMR spectrum of a DBS-CONHNH₂ (6 mM) hydrogel formed in an aqueous solution of pNP (10 mM). Peaks of interest for determining the proportion of mobile and immobile pNP are highlighted.

From the ratios of the peak integrals relating to DMSO and the aromatic pNP protons, the concentration of mobile pNP was calculated as follows:

$$I(\text{DMSO}, 6\text{H}) = 23.02$$

$$I(\text{DMSO}, 1\text{H}) = 3.84 \equiv 0.56 \text{ M}$$

$$I(\text{pNP}, 2\text{H}) = 0.15$$

$$I(\text{pNP}, 1\text{H}) = 0.075 \equiv 0.01 \text{ M} \equiv 10 \text{ mM}$$

10. AP Bioreactor

A hybrid gel ring was prepared as previously reported.¹ The compartment contained within the ring was charged with a solution of pNPP in pH 9 buffer (0.3 mL, 10 mM), whilst the outer compartment contained AP (2 U mg⁻¹, from TCI) dissolved in pH 5.8 buffer (26 U mL⁻¹, 2 mL). The whole reactor was placed in a dark container to prevent light-induced pNPP degradation. The outer compartment was stirred for the duration of the experiment. At each time point, the contents of the outer compartment were removed and diluted to 2 mL using pH 9 buffer (final pH *ca.* 9) and the UV spectrum of the

solution recorded. The product compartment was replenished with fresh pH 5.8 buffer at each time point.

After 6 h, in addition to the removal of the buffer solution, the contents of the central compartment were diluted to 2 mL with pH 9 buffer (final pH *ca.* 9). This solution was also analysed by UV-vis spectroscopy. Calibration curves plotted from absorbances of known concentrations of pNP and pNPP in pH 9 buffer were used to calculate the concentration of these compounds in each compartment.

11. References

1. P. R. A. Chivers and D. K Smith, *Chem. Sci.*, 2017, **8**, 7218-7227.
2. D. J. Cornwell , B. O. Okesola and D. K. Smith, *Angew. Chem., Int. Ed.*, 2014, **53**, 12461-12465
3. J. R. Lakowicz, in *Principles of Fluorescence Spectroscopy*, Plenum Press, New York, London, 1983, p. 44–46.
4. K. Andrieux, P. Lesieur, S. Lesieur, M. Ollivon and C. Grabielle-Madelmont, *Anal. Chem.*, 2002, **74**, 5217–5226.
5. L. Michaelis and M. L. Menten, *Biochem. Z.*, 1913, **49**, 333-369.
6. J. Wang, X. Miao, Q. Fengzhao, C. Ren, Z. Yang and L. Wang, *RSC Adv.*, 2013, **3**, 16739–16746.